10: Detectors in space

Peter Saulson, Syracuse University
with material from
Daniel Shaddock (JPL), Andrea Lommen (Franklin & Marshall), and
the eLISA project

My lectures during this School

1. Overview of gravitational waves and sources
2. Interactions of waves and detectors
3. Shot noise and radiation pressure noise
4. Theory of linear systems
5. Vibration isolation (passive)
6. Thermal noise
7. Optics of Fabry-Perot cavities
8. Feedback control systems
9. Description of LIGO and other current detectors
10. **Future detectors in space**

LIGO and LISA probe different bands of the spectrum

Difference of 10^4 in wavelength:
Like difference between X-rays and IR

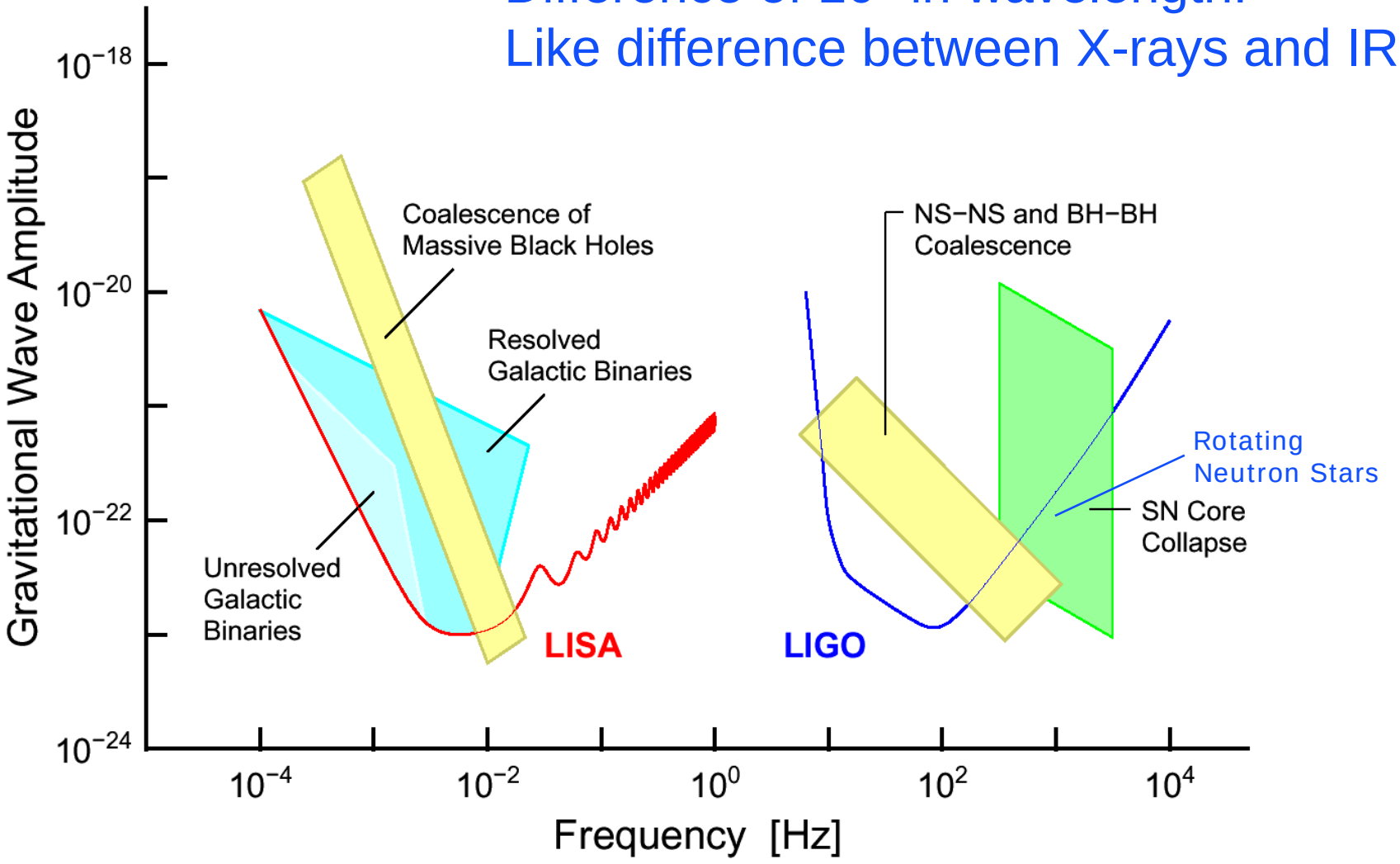

Laser Interferometer Space Antenna Mission: Quick View

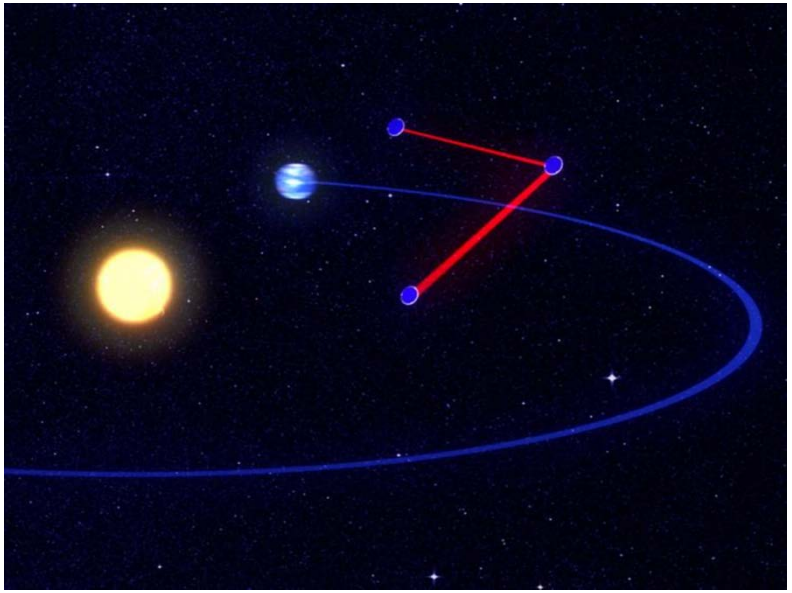

What

- 3 spacecraft constellation separated by 10^6 km.
- Drag-free flight
- Gravitational waves detected as a modulation of the distance between spacecraft by picometer interferometry
- Earth-trailing solar orbit

Why?

- Gravitational radiation from compact binary star systems in our galaxy
- Massive and super-massive black hole mergers
- Gravitational capture of compact stellar objects into massive black holes
- Signatures of gravitational radiation from the early universe

Why go to space?

- Long arms (free vacuum system)
  - Amplifies strain-induced length change
  - Sensitive to lower frequencies, a region rich in gravitational waves.
- Approximates thought experiment-type free masses
  - Low vibration, no seismic noise
  - Excellent thermal stability
  - No gravity gradient noise or “wall”

Sensitivity

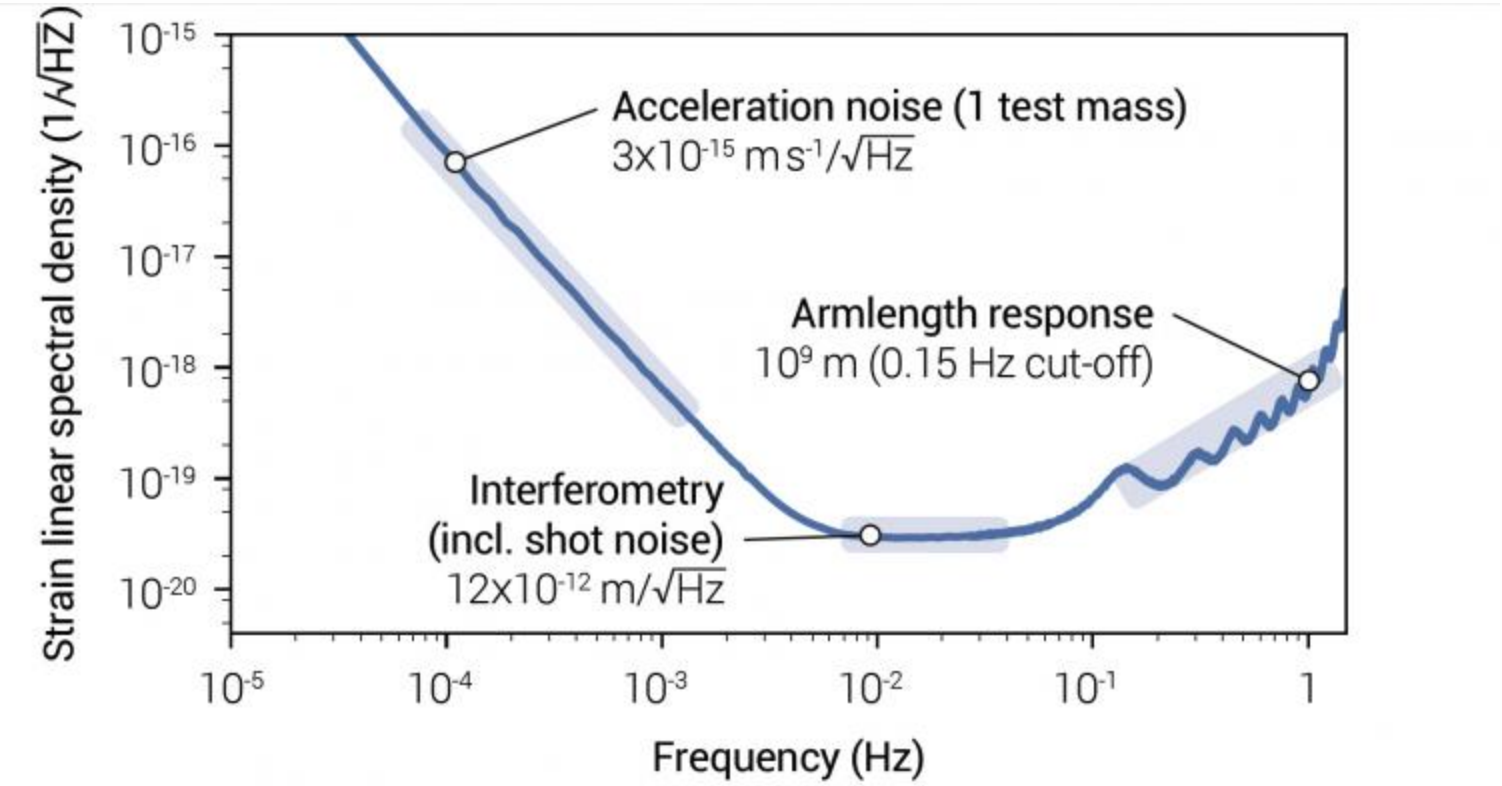

Orbital configuration

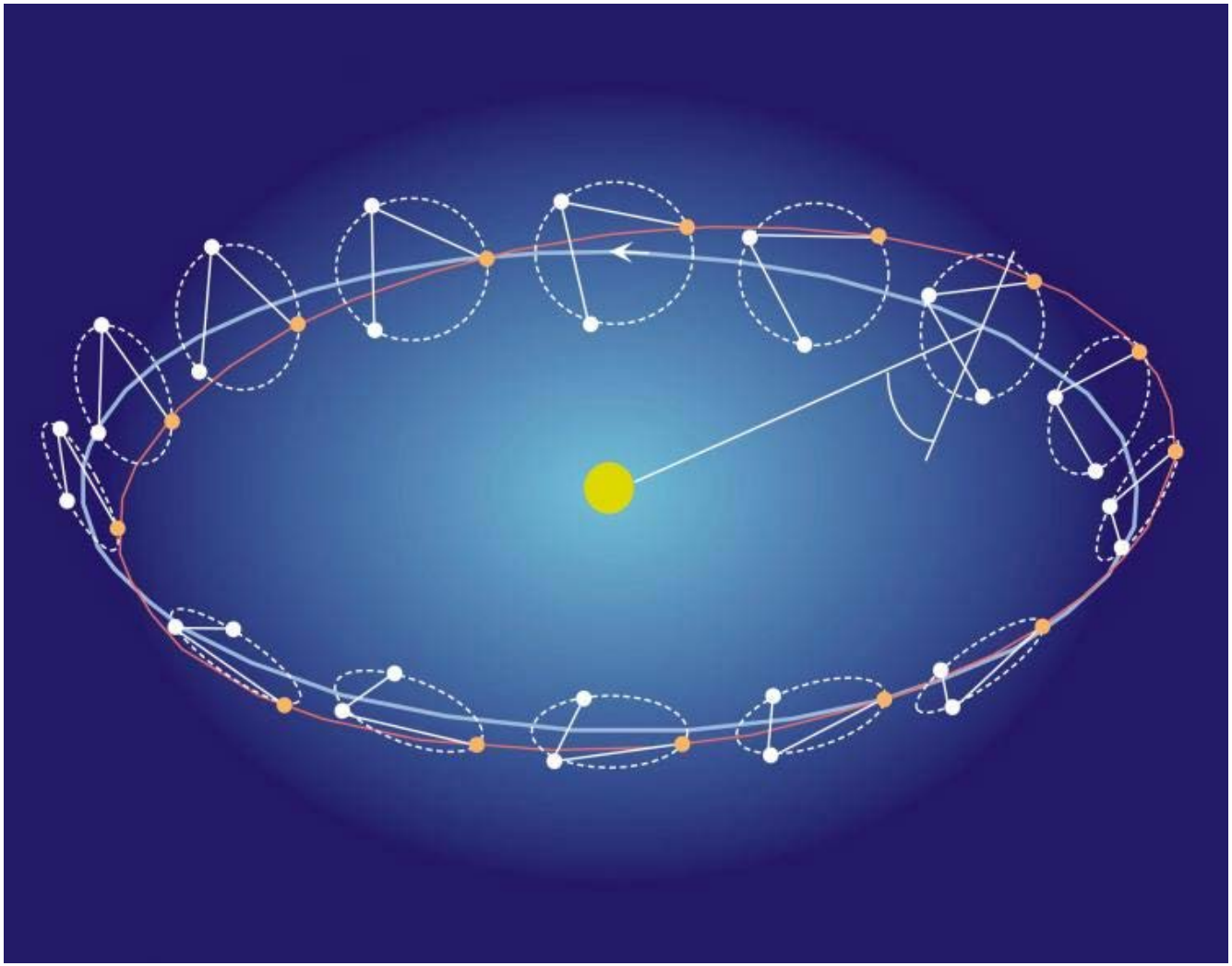

Drag-free operation

Technology Drivers

Inertial sensors

Noise < 10^{-16} g

rms for 1000 s average

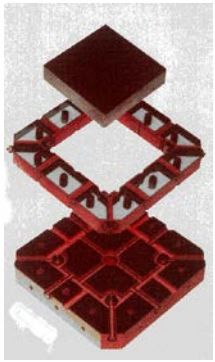

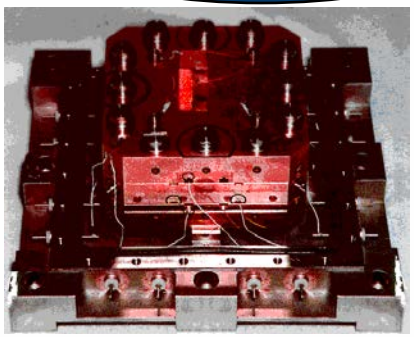

Micro-Newton thrusters

Range 1-100 µN

Noise <1 µN

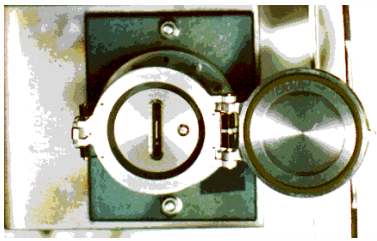

Picometer interferometry

Accuracy < 1 pm

rms for 1000 s average

1 W laser

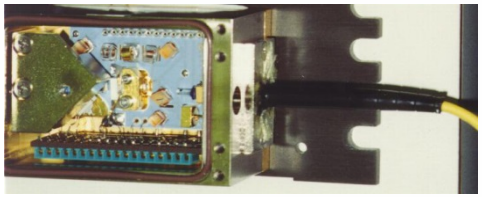

Proof-Mass Capacitive Motion Sensor

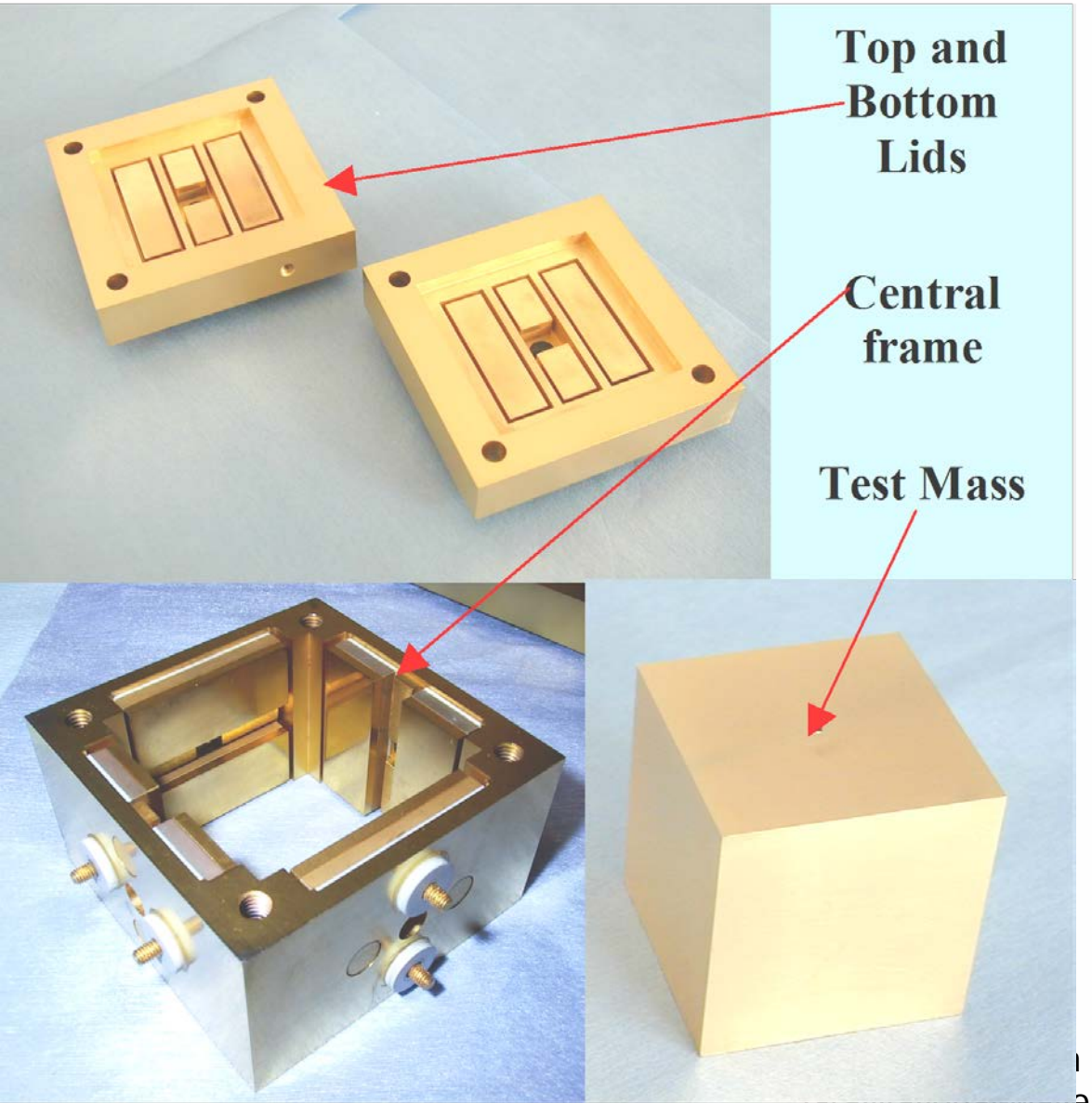

- 6 degrees of freedom
- Minimize thermal gradients
  - metal instead of ULE
- Avoid DC actuation
- Large gaps to reduce patch field effects
- The test masses are 46 mm cubes, made from a dense non-magnetic Au-Pt alloy.

Micro-Newton Thruster Cluster

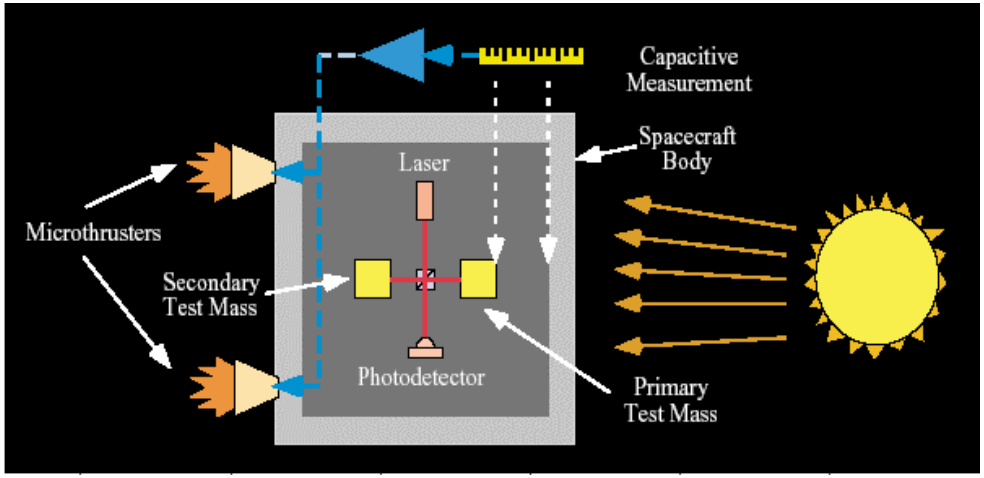

- Colloid Micro-Newton Thrusters balance the solar photon pressure
- "Drag-free" mode, ensures the test masses only feel gravitational forces

ST7/DRS Thruster Cluster

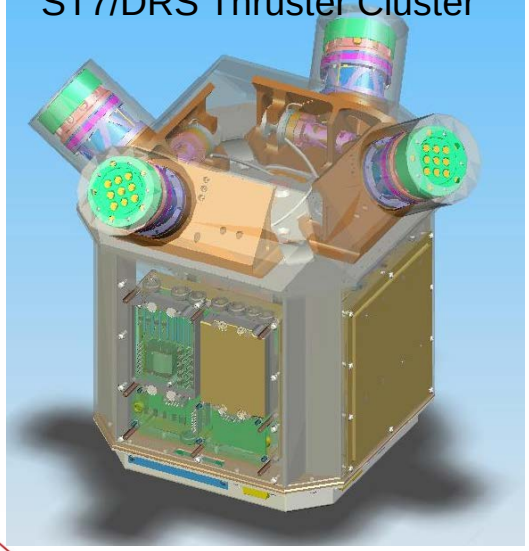

- Each microthruster produces from 5-30 μN with better than 0.1 μN resolution
- A micro-Newton is about one tenth the weight of a grain of sand!

Colloidal thruster (Busek)

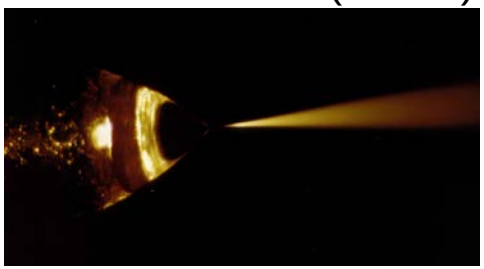

Optical System

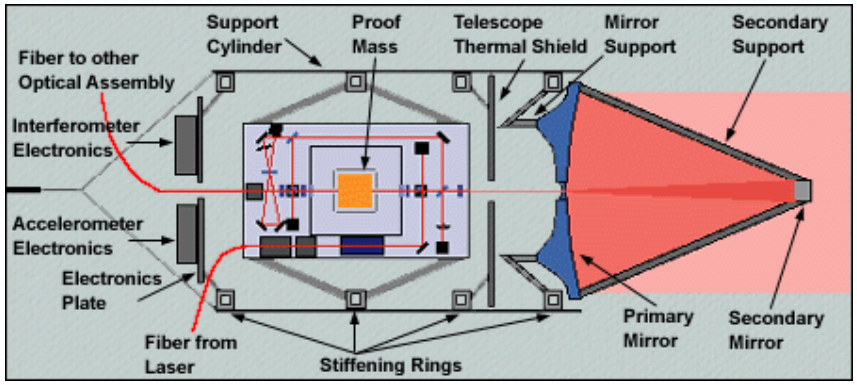

LIGO

1. Optically recombined Michelson interferometer.
2. Optical cavities used to improve shot noise limited sensitivity.
3. Ultra low loss optics (<100 ppm)
4. GW signal proportional to amplitude of heterodyne signal (mixer).
5. <100 μm range

LISA

1. Electronically recombined Michelson interferometer.
2. Phase locked (amplifying) lasers used to improve shot noise limited sensitivity.
3. High diffraction loss (1 W -> 100 pW)
4. GW signal proportional to phase of heterodyne signal (phasemeter).
5. ~10^8 m range

Interferometric laser ranging scheme

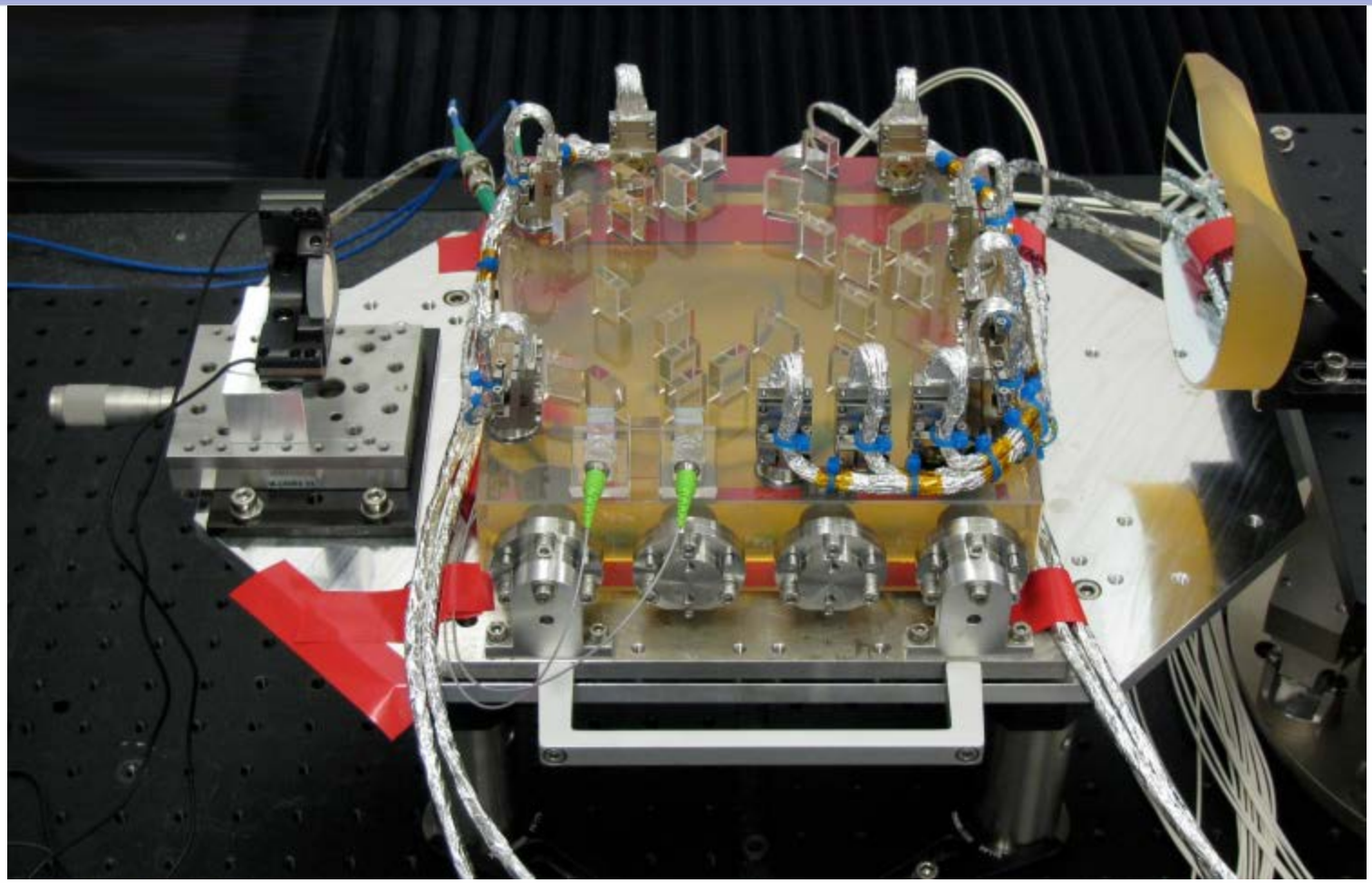

eLISA's version of interferometry

Direct reflection of laser light is **not feasible** due to the large distance between the spacecraft: Diffraction expands the laser beam so much that for each Watt of laser power sent, only about 250 pW are received.

Therefore, lasers at the end of each arm **operate in a "transponder" mode**: A laser beam is sent out from the central spacecraft to an end spacecraft. The laser in the end spacecraft is then phase-locked to the incoming beam thus returning a high-power phase replica. The returned beam is received by the central spacecraft and its phase in turn compared with the phase of the local laser

LISA Path Finder

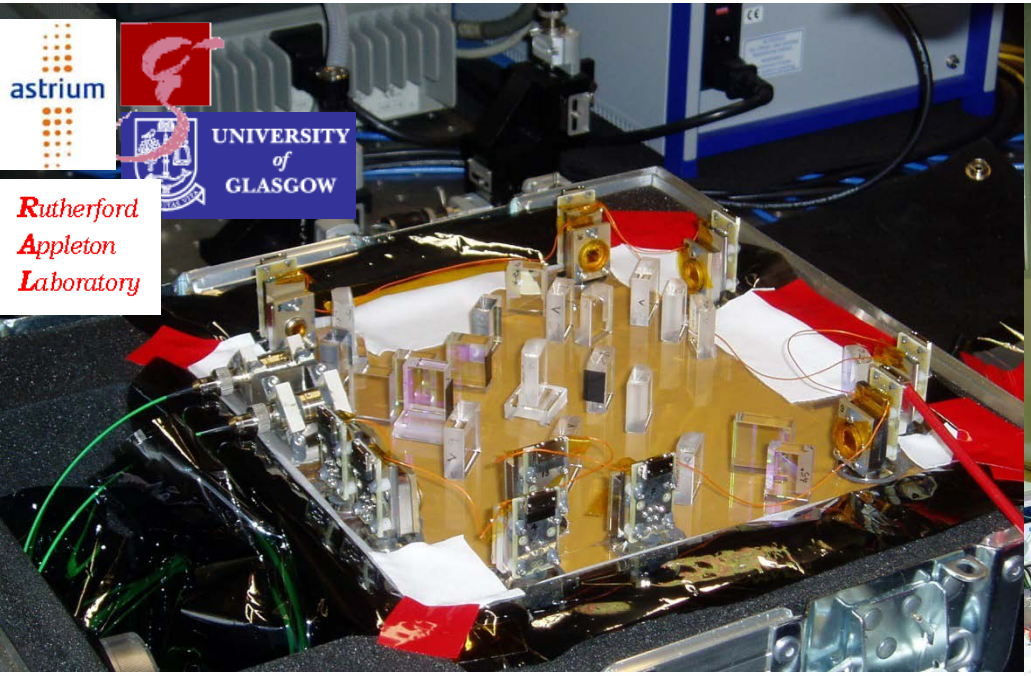

Path Finder EM optical bench

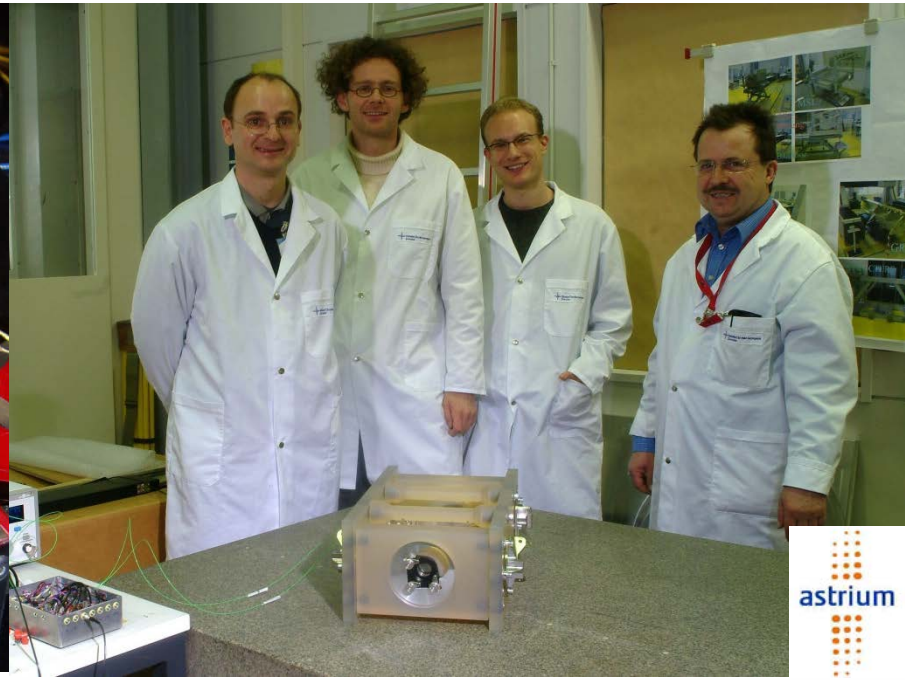

Assembly in Friedrichshafen

Michelson Interferometers

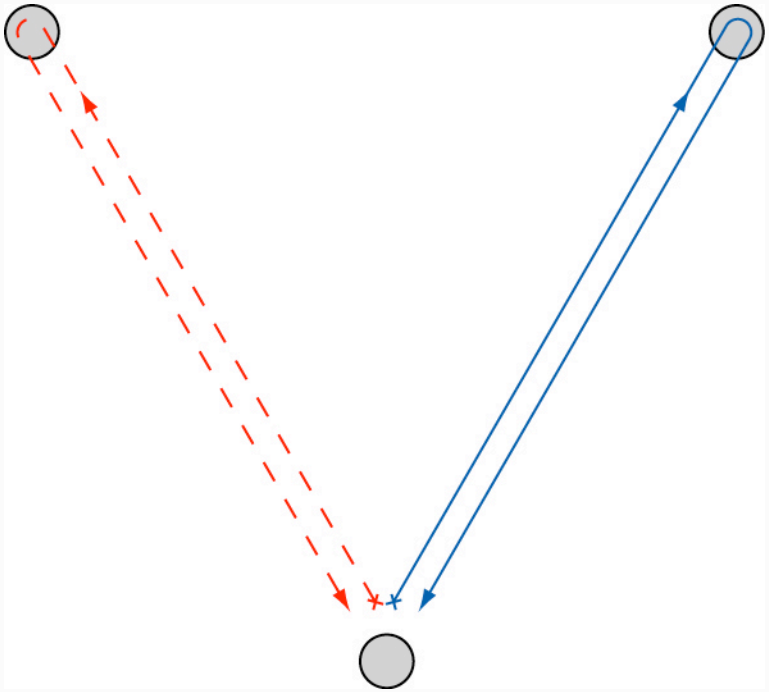

Equal-arm Michelson interferometer

•Insensitive to laser frequency noise

TDI Michelson

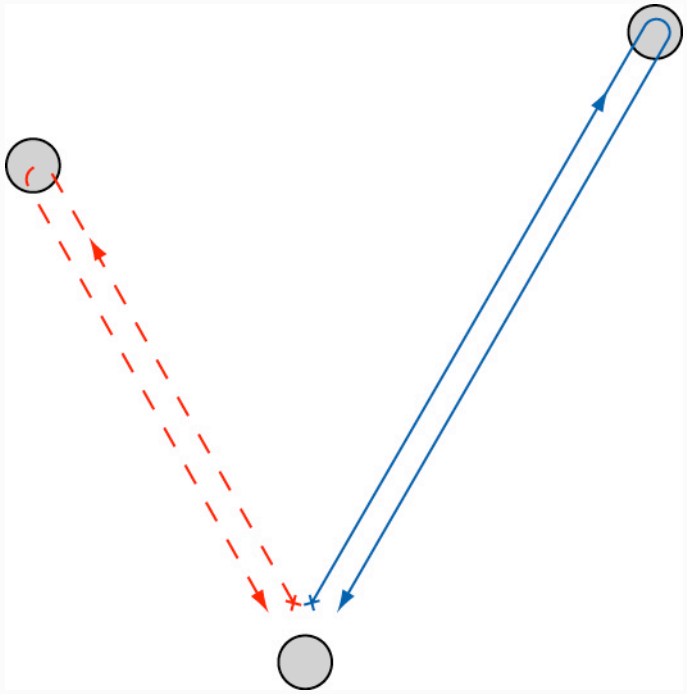

Unequal-arm Michelson interferometer

•Output corrupted by laser frequency noise

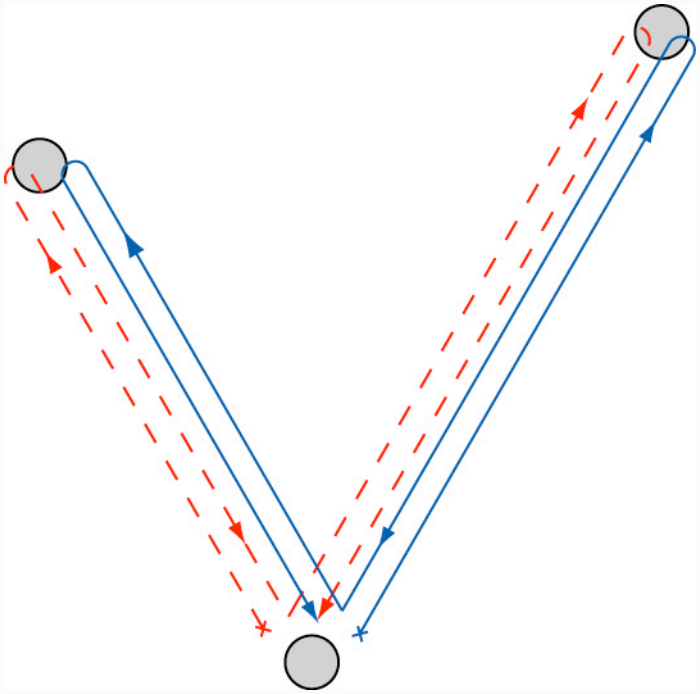

Equal-arm (Sagnac) interferometer (TDI combination X)

•Output immune to laser frequency noise

Sagnac Interferometer

Counter-propagating beams traverse the same optical path.

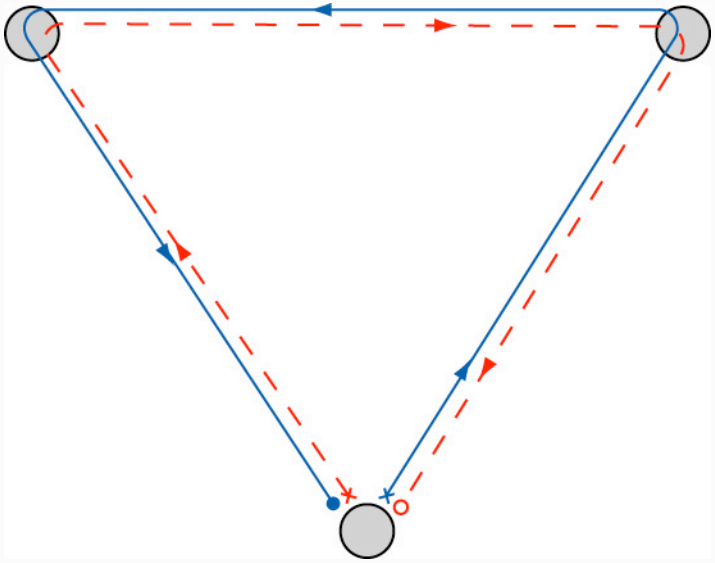

Equal arm Sagnac interferometer (TDI combination α)

•Output immune to laser frequency noise

TDI with spacecraft motion

- In the presence of constant rotation a path length difference between the clockwise and counter-clockwise propagating beams is introduced.

$$\Delta L \equiv L_{CW} - L_{CCW} = \frac{4\Omega \cdot A}{c}$$

Where Ω is the angular rotation, A is the area enclosed, and c is the speed of light. The area of an equilateral triangle is,

$$A = \frac{L^2\sqrt{3}}{4}$$

Assuming L=5x10^9 m and Ω=1 cycle/year (2x10^{-7} rad/sec) we have,

$$\boxed{\Delta L = 14.4 \text{ km}}$$

Note: the rotation vector is not normal to the plane of the interferometer and so $\Omega \cdot A = \frac{|\Omega||A|}{2}$

D.A. Shaddock, *Operating LISA as a Sagnac interferometer,* Phys. Rev. D **69**, 022001 (2004).

New Sagnac combination α_1

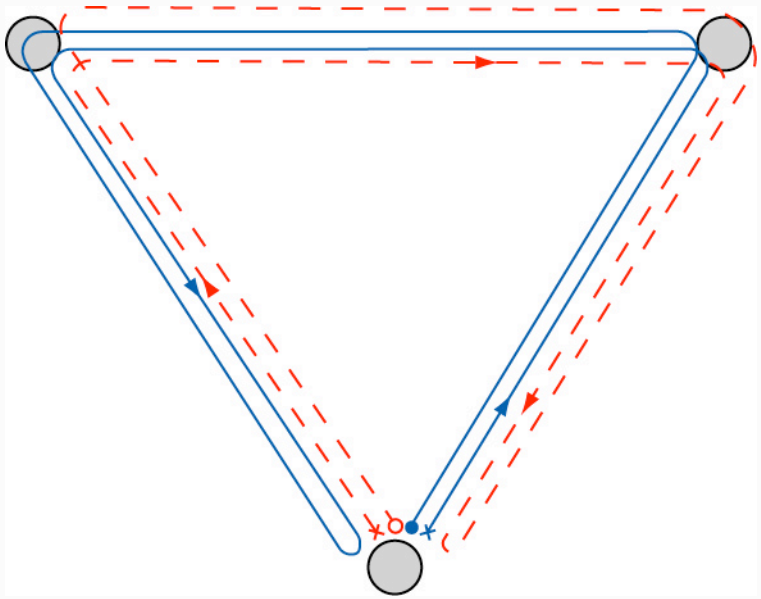

- α_1 Sagnac combination recovers immunity to laser frequency noise.
- First of the “second generation” TDI combinations.

D.A. Shaddock, *Operating LISA as a Sagnac interferometer*, Phys. Rev. D **69**, 022001 (2004).

TDI Michelson with S/C motion

Constant spacecraft velocity introduces an arm length mismatch to the synthesized interferometer.

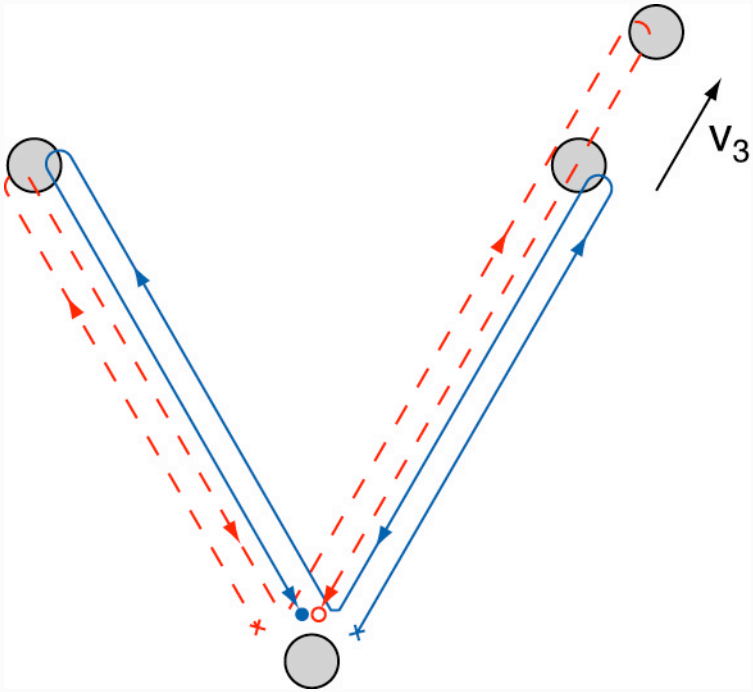

This arm length mismatch could be as much as

ΔL ~ 20m/s x 33 s

~ 660 m

N.J. Cornish and R.W. Hellings, *The effects of orbital motion on LISA time delay interferometry*, Class. Quantum Grav. **20**, 22 4851 (2003)

2nd Gen TDI Michelson X_1

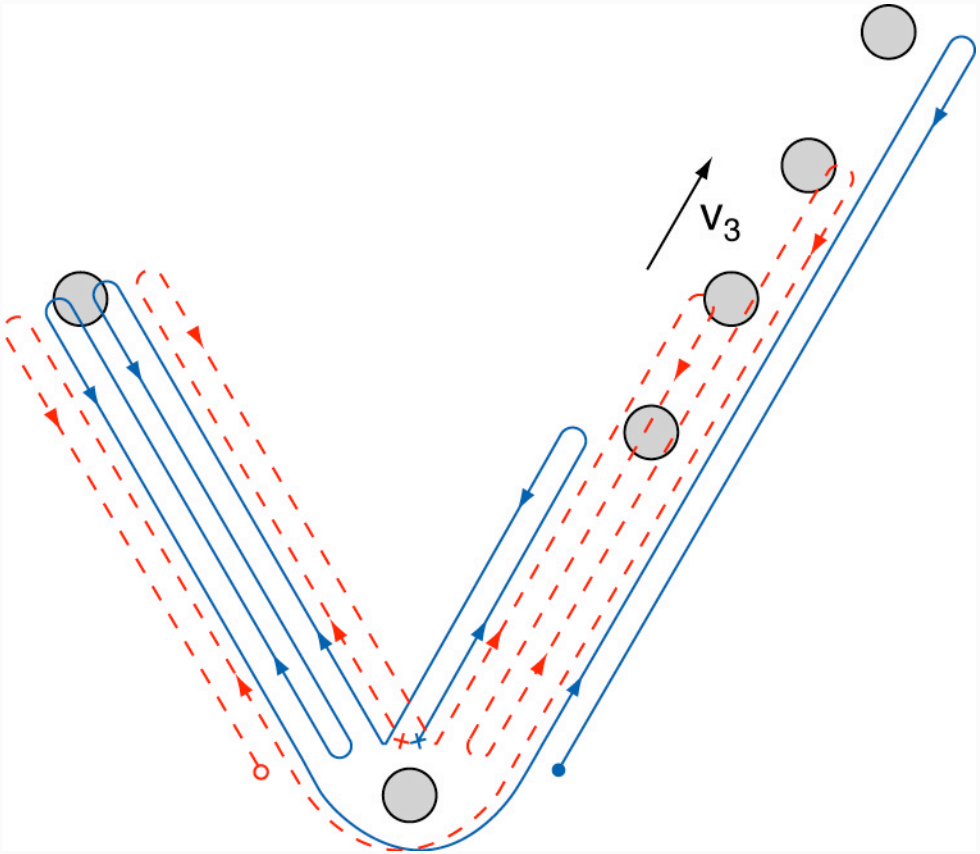

D.A. Shaddock, M. Tinto, F.B. Estabrook, J.W. Armstrong, *Data combinations accounting for spacecraft motion,* Phys. Rev. D **68**, 061303 (2003).

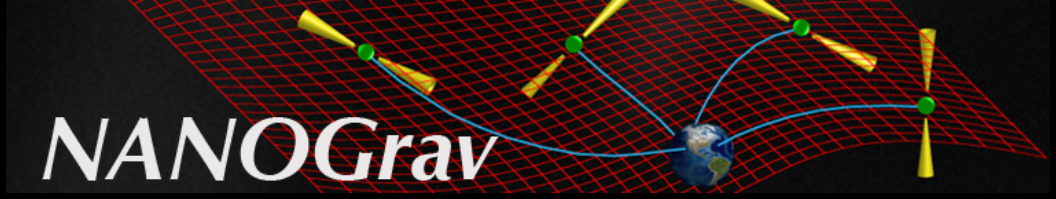

The International Pulsar Timing Array

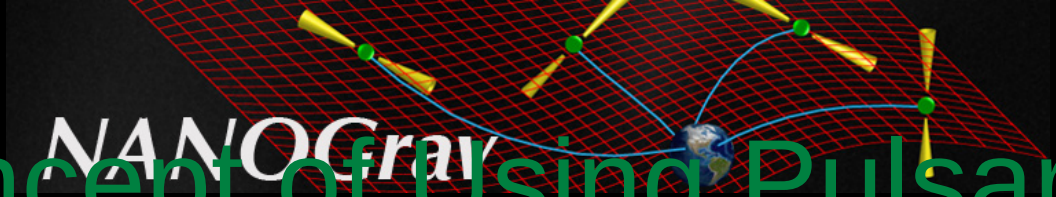

Concept of Using Pulsars to Detect Gravitational Radiation

- Imprint on Pulsar timing residuals
  - Sazhin 1978
- Explicit connection between Doppler data from spacecraft and pulsar timing data
  - Detweiler 1979
- Concept of a Pulsar Timing Array
  - Foster and Backer 1990
- First limit on stochastic GW background
  - Stinebring, Ryba, Taylor, & Romani 1990

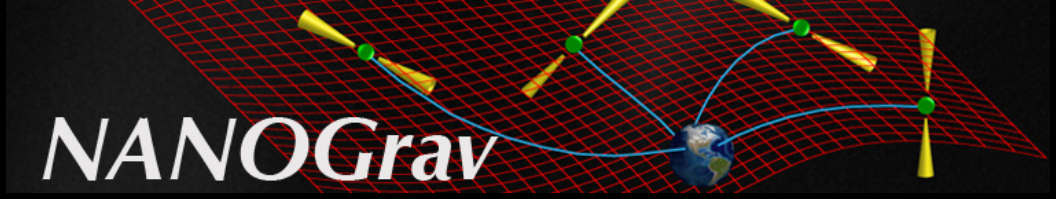

Stability of the clocks

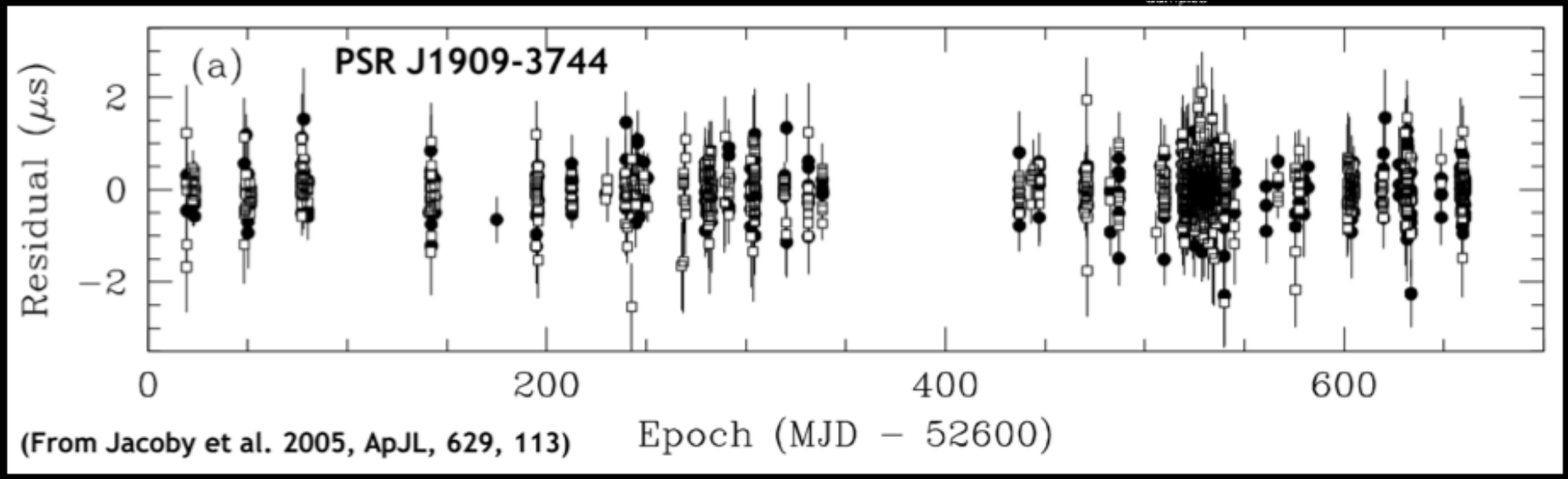

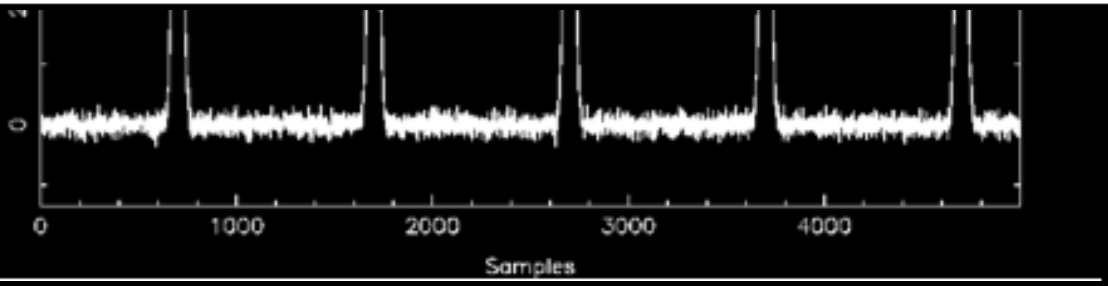

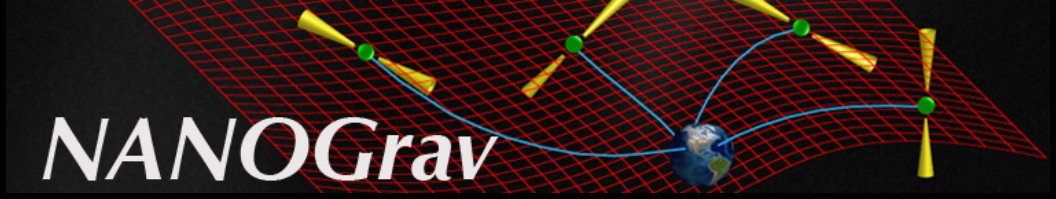

Orbital Motion in the Radio Galaxy 3C 66B: Evidence for a Supermassive Black Hole Binary **Sudou, Iguchi, Murata, Taniguchi (2003) Science 300: 1263-1265.**

Constraining the Properties of Supermassive Black Hole Systems Using Pulsar Timing: Application to 3C 66b**, Jenet, Lommen, Larson and Wen (2004) ApJ 606:799-803.**

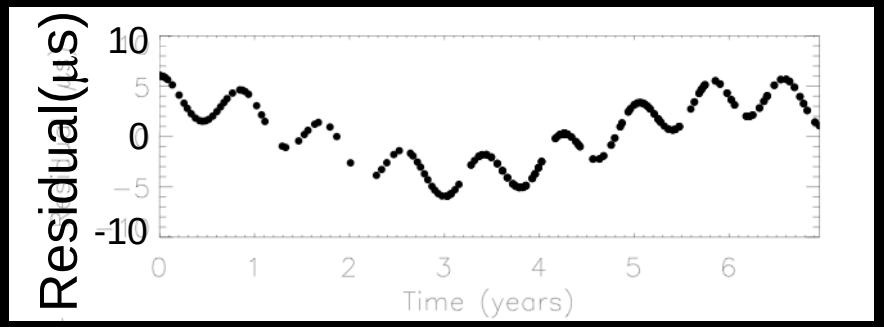

Simulated residuals due to 3c66b

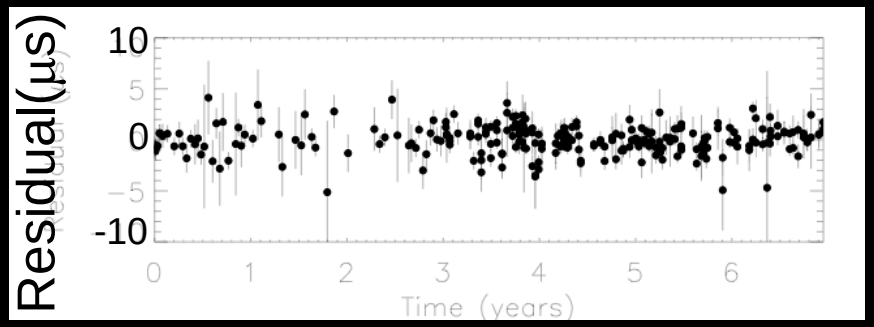

Data from Kaspi, Taylor, Ryba 1994

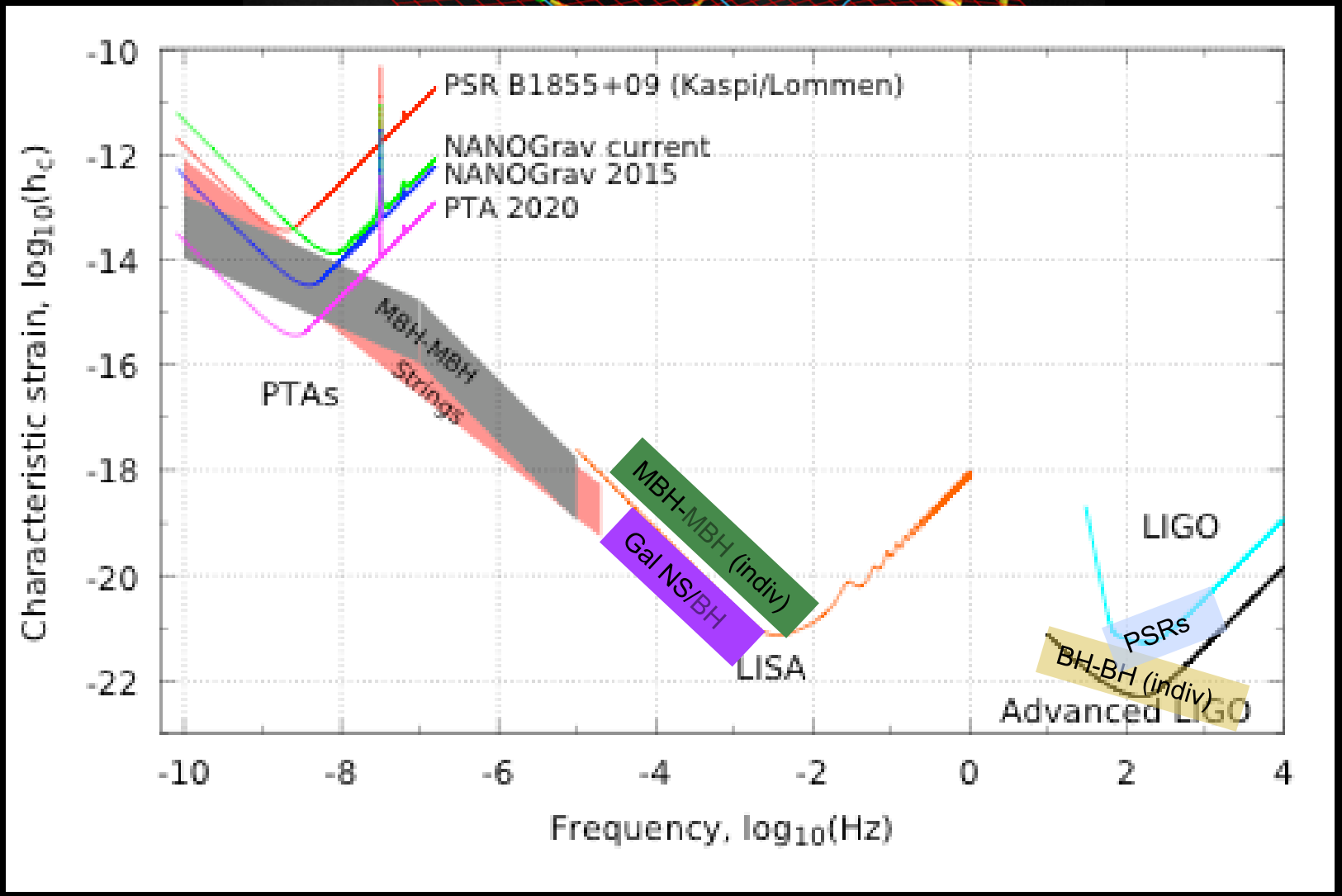

Figure by Paul Demorest (see arXiv:0902.2968)